Article

pubs.acs.org/Biomac

Intrinsically Fluorescent PAMAM Dendrimer as Gene Carrier and Nanoprobe for Nucleic Acids Delivery: Bioimaging and Transfection Study

Ya-Ju Tsai,[†] Chao-Chin Hu,[†] Chih-Chien Chu,*[,†,‡] and Toyoko, Imae[§]

[†]School of Applied Chemistry, Chung Shan Medical University, Taichung 40201, Taiwan

[‡]Department of Medical Education, Chung Shan Medical University Hospital, Taichung 40201, Taiwan

[§]Graduate Institute of Applied Science and Technology, National Taiwan University of Science and Technology, Taipei 10607, Taiwan

Supporting Information

ABSTRACT: This study successfully evaluated gene delivery and transfection toward rat C6 glioma cell lines mediated by intrinsic blue fluorescent poly(amido amine) (PAMAM) dendrimer. We used three antisense oligonucleotides, (AS-ODN) p75, NGF1, and NGF2 for knocking down specific protein expressions. The three oligonucleotides were electrostatically associated with the photoluminescent amino-terminated PAMAM dendrimer to yield fluorescent complexes at various nitrogen-to-phosphorus (N/P) ratios. Compared with pristine PAMAM dendrimer and hyperbranched polyethylenimine (PEI), the fluorescent PAMAM dendrimer revealed lower in vitro cytotoxicity toward C6 cells, allowing us to transfect the cells with the AS-ODN complexes under a higher N/P ratio. Due to the intrinsic fluorescence, cellular uptake behavior could be directly analyzed by fluorescence microscopy and flow cytometry, without additional fluorescence labeling. As expected, the result clearly suggested that the uptake efficiency increased as the N/P value increased. Furthermore, the quantified data obtained from flow cytometry indicated relatively higher uptake efficiency for the p75 complex, which is mainly due to different association patterns between the fluorescent dendrimer and AS-ODNs. At N/P = 20, atomic force microscopic analysis confirmed that the p75 complex formed well-condensed, spherical particles with dimensions less than 200 nm, but that NGF2 AS-ODN associated poorly with the dendrimer. Finally, Western blot analysis indicated that these complexes were capable of knocking down the specific protein expression to a certain level, being comparable to the hyperbranched PEI-mediated gene transfection. Our preliminary results clearly indicated that intrinsic fluorescent PAMAM dendrimers show promise as gene vehicles that can achieve delivery, transfection, and bioimaging at the same time.

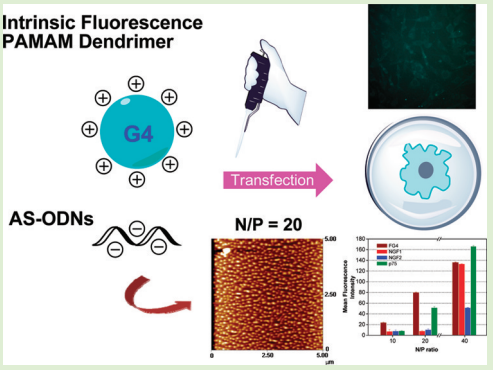

INTRODUCTION

Antisense technology in which sequence-specific DNA and RNA molecules down-regulate ("knock down") the expression of disease-causing proteins has aroused great interest in recent years.[1−3] Particularly, through rational design, antisense oligonucleotides (AS-ODN) and small interfering RNA (siRNA) are able to inhibit expression of specific genes by either interfering with the translation or by inducing the cleavage of target mRNA.[4] Despite the obvious promise shown by nucleic acids as gene-therapeutic agents, in clinical practice there are barriers to using AS-ODN and siRNA. The main barrier is their instability in physiological fluid and their poor penetration into cells. Therefore, developing an efficient delivery system remains a major challenge for the wide clinical application of antisense technology.[5] Among all the polymer-based vectors toward nucleic acid delivery, poly(amido amine) (PAMAM) dendrimers, which have been considered as biocompatible, nonimmunogenic, and water-soluble gene vehicles, demonstrated remarkable in vitro transfection efficiency of plasmid DNA;[6−10] nevertheless, their ability to knock down gene expression through antisense strategies requires more investigation.[11−15]

Full-generation PAMAM dendrimer bears multiple primary amines on the surface and internal tertiary amines as branching sites. The peripheral amines allow the formation of nanoscaled polyplexes of DNA and the PAMAM dendrimer through electrostatic interaction, thus, promoting cellular uptake efficiency. The internal tertiary amines act as a proton sponge in the acidic endosomes, leading to the release of DNA into the cytoplasm.[16] However, amine-terminated PAMAM dendrimers usually suffer from concentration and generation-dependent cytotoxicity because a high density of cationic amine groups may induce cell apoptosis. Partial surface modification with acetyl groups or with poly(ethylene glycol) (PEG) is adopted

Received: August 26, 2011
Revised: October 25, 2011
Published: October 27, 2011

to decrease the overall positive charges, hence, reducing the cytotoxicity of the PAMAM dendrimer.[17−19]

In evaluating the biological function in vitro or in vivo, covalent attachment of the fluorescent labels onto either nucleic acids or dendritic scaffold is often required, because the pristine PAMAM dendrimer is a nonfluorescent macromolecule.[20−22] However, the modification of organic fluorophores may risk decreasing biocompatibility and affect the size and mobility of the dendrimer.[23] Recent research has described the inherent blue photoluminescence originating from PAMAM dendrimer and found that the emission intensity could be dramatically enhanced with oxidative treatments (using, for example, oxygen and oxidizing agents).[24,25] Furthermore, this unusual emission behavior exhibits generation and pH dependency. Recently, Jasmine et al. reported that controlled aggregation of dendrimer units also results in many-fold enhancements in the intrinsic emission.[26,27] Although the inherent fluorescent PAMAM dendrimer (without fluorophore conjugation) seems to be a promising candidate for straight monitoring the dendrimer-based delivery of gene therapy, to date relatively little research has explored this area.[28−31]

In the current study, we demonstrated the use of fluorescent PAMAM (F-PAMAM) dendrimer as a gene carrier to deliver antisense oligonucleotides (AS-ODN), to inhibit either p75 neurotrophin receptor (p75NTR) or nerve growth factor (NGF) in rat C6 glioma cells.[32] The emission intensity of F-PAMAM dendrimer remained unaffected before and after the electrostatic complexation with AS-ODN at various nitrogen-to-phosphorus (N/P) ratios. Therefore, intracellular uptake efficiency of the complexes was observed by fluorescence microscopy and quantified by flow cytometry, in which more than 99% of cells were positive to the fluorescent complex when transfected at optimized N/P values. Moreover, Western blotting analysis confirmed that both p75NTR and NGF protein expression could be effectively down-regulated in the cells that had shown higher uptake efficiency. Our results clearly indicated a multiple function of F-PAMAM dendrimer that achieves delivery, transfection, and bioimaging at the same time.

EXPERIMENTAL SECTION

Materials. From Sigma-Aldrich (U.S.A.) we purchased G4 amine-terminated PAMAM dendrimer (10 wt % in methanol), hyperbranched polyethylenimine (PEI, M_w = 25000 Da), 3-(4,5-dimethylthiazol-2-yl)-2,5-diphenyltetrazolium bromide (MTT), ammonium persulfate (APS), dimethylsulfoxide (DMSO), formaldehyde, sodium orthovanadate, phenylmethylsulfonyl fluoride (PMSF), and trishydroxymethyl aminomethane (Tris). From Bio-Rad (U.S.A.) we obtained sodium dodecyl sulfate (SDS), bisacrylamide, *N*,*N*,*N*,*N*-tetramethyl ethylenediamine (TEMED), and nitrocellulose (NC) membrane (0.45 μm). Minimal essential medium (MEM), phosphate buffer saline (PBS), fetal bovine serum (FBS), ethylenediaminetetraacetic acid (EDTA), penicillin, glutamine, and streptomycin were purchased from Gibco (U.S.A.). Fluorescent PAMAM dendrimer was prepared following the published procedure.[24] Fresh PAMAM dendrimer solution (0.2 mL) was diluted with distilled water (2.6 mL) and then promptly treated with 0.1 M APS solution (0.2 mL). The mixture was stirred at room temperature for 12 h and then diluted with water (13 mL) to yield a fluorescent dendrimer solution as a stock solution (~1 μg/μL). The phosphorothioate oligonucleotides obtained from GenScript (U.S.A.) were used according to the published sequence for rat p75NTR and rat NGF: p75 antisense (bp 108−122: 5′-CCTCCTCATTGCACG-3′), NGF1 antisense (bp 284−298: 5′-CATGGACATTACGCT-3′), and NGF2 antisense (bp 690−704: 5′-CACTGTCACACACTG-3′).[32] All AS-ODN sequences were dissolved in distilled water and stored at −20 °C.

Characterization of PAMAM Dendrimers and Complexes. Nuclear magnetic resonance (NMR) spectra were recorded on a Varian Mercury Plus 400 MHz spectrometer, at room temperature using D_2O as solvent and tetramethylsilane (TMS) as internal standard. Spectral processing (Fourier transform, peak assignment, and integration) was performed using MestReNova 6.2.1 software. The UV−vis and fluorescence spectra were performed on a Molecular Devices FlexStation 3 microplate reader. For atomic force microscopic (AFM) analysis, 5 μL of each sample was placed on a freshly cleaved mica sheet. After a 5 min incubation at room temperature, the sheet was washed twice with 100 μL of double-distilled H_2O. The prepared samples were first dried from the edge of the mica sheet using a paper tissue and then by exposure to gentle air flow for 10 min. The samples were then immediately subjected to AFM study. We used a Nanoscope IIIa Multimode scanning probe microscope from Digital Instruments (Veeco Metrology Group, Santa Barbara, CA) in contacting mode with a scan rate of 2.441 Hz and a tip velocity of 2.35 μm/s. Analyses of the images were carried out using the Nanoscope III software version 5.31R1.

Cell Culture and In Vitro Gene Transfection. Rat C6 glioma cell line was obtained from the American Type Culture Collection (ATCC, Manassas, VA). Cells were cultured in minimal essential medium supplemented with 5% fetal bovine serum and antibiotics (1% penicillin and 100 mg/mL streptomycin) at 37 °C, in a humidified atmosphere of 5% CO_2 (v/v) in air.

Prior to transfection, cells were seeded in 6 cm dishes at a density of 1.5×10^5 cells per dish, in a complete medium (MEM, FBS, and antibiotics). After incubation for 24 h, the cells were removed from the complete medium, washed with PBS buffer solution, and fed with serum-free medium (2.8 mL/dish). Meanwhile, 100 μL of dendrimer solution, ranging from 173 to 692 μg/mL, was mixed in serum-free medium with 100 μL of AS-ODN solution (50 μg/mL). The mixtures with a total volume of 0.2 mL were agitated thoroughly to result in electrostatic complexes with specific N/P ratios of 10, 15, 20, and 40, where the dendrimer concentration equals 6.1, 9.1, 12, and 24 μM, respectively. The prepared solutions were incubated at room temperature for 30 min and then added into the respective dishes of cells. After incubation at 37 °C for 12 h, the transfection medium was replaced with the complete medium, and the cells remained in culture for another 72 h before being harvested for flow cytometry and Western blot analysis.

In Vitro Cytotoxicity Assay. A modified MTT assay was used to assess in vitro cytotoxicity of the dendrimers toward C6 glioma cell lines. Prior to cytotoxicity measurement, cells were grown in a 24-well plate at a density of 3×10^4 cells per well. After incubation for 24 h, dendrimers were added into each well to attain the final concentration from 0.36 to 5.6 μM. After incubation at 37 °C for 12 h, MTT solution (0.5 mg/mL) was added and the mixture was incubated for another 4 h; subsequently, the solution was replaced with DMSO (1 mL) to dissolve the formazan crystal formed by live cells. Following the transfection protocol described above, the cytotoxicity of the cells transfected by the dendrimer−oligonucelotide complexes at various N/P ratios was measured by the same MTT procedure. The viability of the cells was determined by visible absorbance at 540 nm using an ELISA plate reader (EL-800, BioTek, U.S.A.). Four independent experiments were performed, and each experiment was done in triplicate. The data points shown in Figures 2 and 4 were expressed as mean ± standard deviation.

Fluorescence Microscopy and Flow Cytometry. Cells were cultured and transfected following the procedures outlined above. After incubating for 12 h at 37 °C, the cells were washed three times with cold PBS buffer solution and then fixed by the addition of 300 μL of formaldehyde (3.75% v/v PBS solution), and were then left to stand for 35 min. Cells were washed three times with cold PBS buffer solution and then mounted directly onto glass microscope slides using Fluorescent Mounting Medium (Dako, U.S.A.), sealed with clear nail polish, and processed for upright fluorescence microscopy (Axioskop 2, ZEISS, Germany) with external irradiation lamp at 365 nm.

Following the transfection protocol described above, the cells were washed twice with PBS buffer solution and a single cell suspension was

prepared by trypsinization. After this a total of 10,000 nuclei were examined with a FACSCalibur flow cytometer (Becton Dickinson Immunocytometry System, UK) equipped with an argon laser (488 nm emission wavelength); cell fluorescence was detected in the FL2 channel (wavelength: 585 nm; bandwidth: 42 nm) and the number of positive cells and mean fluorescence intensity were counted. The data obtained were analyzed with WinMDI software. Each data shown in Figure 6 was expressed as mean ± standard deviation of three experiments.

Western Blotting Analysis. The cells were harvested following the transfection protocol described above. To prepare the whole-cell extract, cells were washed with PBS buffer solution containing 1 mM of zinc ion and then suspended in a lysis buffer solution (pH = 7.5) containing 50 mM Tris, 5 mM EDTA, 150 mM NaCl, 1% NP40, 0.5% deoxycholic acid, 1 mM sodium orthovanadate, 81 μg/mL aprotinine, 170 mg/mL leupeptin, and 100 mg/mL PMSF. After incubation at 4 °C for 30 min, the mixtures were centrifuged at 10000 g for 10 min, and the supernatants were collected as whole-cell extracts. The protein concentration of the whole-cell extracts was determined by Bio-Rad protein assay reagent. A total of 25 μg of whole-cell extracts were then separated by 8−12% SDS-PAGE and transferred onto NC membrane. After blocking with 5% nonfat milk, the membrane was incubated with primary antibody at 4 °C overnight and then washed with 0.1% Tween-20/PBS solution. It was then incubated with peroxidase-conjugated secondary antibody. The signal was detected by enhanced chemiluminescence substrate and captured with a chemiluminescence recorder (LAS-1000, Fujifilm). The primary antibodies used in this study were as follows: anti-NGF, anti-p75 (both used at 1:1000 dilution), and anti-β-actin (used at 1:3000 dilution; Santa Cruz Biotechnology, U.S.A.).

RESULTS AND DISCUSSION

Fluorescence Properties of F-PAMAM Dendrimers and AS-ODN Polyplexes. NH_2-terminated PAMAM dendrimer has been known to form a stable complex with oligonucleotides at a defined N/P ratio. The current study sought to understand the action of intrinsically fluorescent PAMAM (F-PAMAM) dendrimer in the delivery of AS-ODN into cells. Fresh G4 PAMAM dendrimer with multiple positive charges, but negligible inherent fluorescence, was readily treated with excess ammonium persulfate (APS) to enhance fluorescence intensity through the oxidation procedure. Because excess APS gradually decomposed in aqueous solution with the evolution of abundant oxygen, the oxidation of PAMAM dendrimer could be accelerated and, thus, the fluorescence intensity effectively increased within hours.[33−35] The electrostatic complexation of thus-prepared F-PAMAM dendrimer and negatively charged AS-ODN was then carried out by simply mixing the two components thoroughly in water. Figure 1 shows the excitation (λ_{max} ~ 380 nm) and emission (λ_{max} ~ 460 nm) spectra of the F-PAMAM/AS-ODN (p75) complexes at various N/P ratios, where N and P represent the number of nitrogen and phosphorus groups, respectively, on the dendrimer and oligonucleotides. The fluorescent profiles of these electrostatic complexes were quite similar to those of uncomplexed F-PAMAM dendrimers and obeyed a concentration dependency such that the intensity gradually increased as the N/P ratio increased.

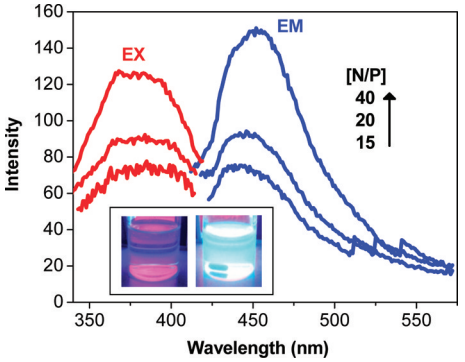

Figure 1. The excitation (EX) and emission (EM) spectra of the electrostatic complexes composed of ammonium persulfate-treated PAMAM dendrimer and p75 antisense oligonucleotides (AS-ODN), at various nitrogen-to-phosphorus (N/P) ratios, namely 15, 20, and 40 (λ_{ex} = 380 nm, λ_{em} = 460 nm). Inset: the visualized images of the PAMAM dendrimers before (left) and after (right) oxidative treatment.

Jasmine et al. have reported significant fluorescence enhancement of the electrostatically assembled carboxylate and amine-terminated PAMAM dendrimers; however, association between cationic F-PAMAM dendrimers and anionic AS-ODN is unable to intensify the emission. This finding is ascribed to two possible reasons: (i) the F-PAMAM/AS-ODN complexes usually form compact spherical nanoparticles rather than ordered fractal microaggregation composed of the dendrimers with opposite charges, which is insufficient to reduce the exciton quenching through a nonradiative pathway; (ii) oxidation via APS treatment (in comparison with air or oxygen process) allows the fluorescence intensity to be saturated within several hours, thus, electrostatic complexation cannot further enhance emission. Although the mechanistic details of the intrinsic emission remain intriguingly mysterious to date, it has been proposed that the fluorescence property originates from the interior amino-branching sites, and that oxidative treatment is essential in this nonclassical emission behavior.[36,37] Notably, the F-PAMAM/AS-ODN complexes without fluorescence probe labeling have revealed blue photoluminescence (see inset in Figure 1), which can be used to directly study the subcellular distribution of these dendrimer−oligonucleotide complexes.

In Vitro Cytotoxicity of F-PAMAM Dendrimers and F-PAMAM/AS-ODN Complexes. Prior to cellular uptake and transfection experiments, a modified MTT assay was adopted to access the cytotoxicity of F-PAMAM dendrimers.[38] It is known that in vitro cytotoxicity for PAMAM dendrimers depends on the concentration, peripherals, and type of cell lines. Generally, the NH_2-terminated PAMAM dendrimer due to the high density of surface positive charges was more toxic than OH-terminated and surface-acetylated PAMAM dendrimers, but possessed much higher cellular membrane permeability. Figure 2 shows the viability of C6 glioma cells incubated with different concentrations of G4 PAMAM and F-PAMAM dendrimers for 12 h. The C6 cells exhibited a great sensitivity when exposed to NH_2-terminated PAMAM

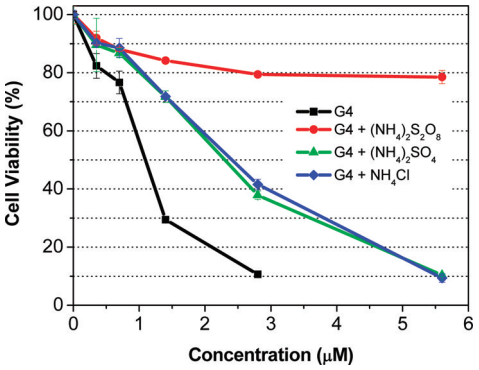

Figure 2. In vitro cytotoxicity analyses for pristine G4 NH_2-terminated PAMAM dendrimer (■), and for the dendrimer treated with $(NH_4)_2S_2O_8$ (●), $(NH_4)_2SO_4$ (▲), and NH_4Cl (◆). The results are expressed as percentage of cell viability relative to untreated rat C6 glioma cells. Data are the mean ± standard deviation of four experiments, each conducted in triplicate.

dx.doi.org/10.1021/bm201196p | Biomacromolecules 2011, 12, 4283−4290

dendrimer, and viable cells were hardly detected under the dosage of 5.6 μM. This result is consistent with a previous report that higher generation G5 and G7 NH_2-terminated PAMAM dendrimers revealed even higher toxicity toward C6 cell lines.[39] Moreover, we found that hyperbranched PEI, one of the most highlighted gene vectors, also exhibited acute toxicity (Figure S1). This finding confirmed that the cationic polymers, bearing abundant amino groups within the structure, easily triggered C6 cell death. Interestingly, F-PAMAM dendrimer was much less toxic for C6 cells, and over 80% of cells were still viable under the same dosage. This substantial decrease in toxicity has also been observed for surface-acetylated PAMAM dendrimer, in which the end-group-modification from primary amines to acetamides reduced the surface cationic charges and cytotoxicity.[12]

However, the chemical structures for F-PAMAM and pristine PAMAM dendrimer, as analyzed by ^{1}H NMR (Figure 3),

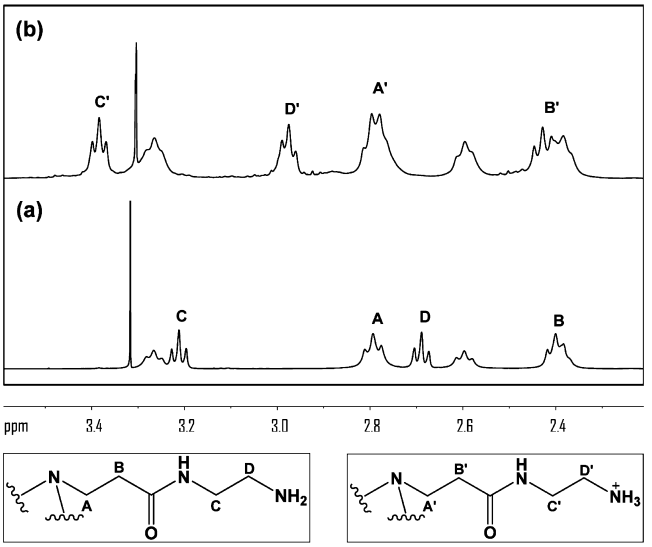

Figure 3. ^{1}H NMR spectra of NH_2-terminated PAMAM dendrimer before (a) and after (b) oxidative treatment. The peripheral methylene protons were assigned as A∼D and A′∼D′, corresponding to the chemical structures shown below.

revealed only one distinguishable difference that all the outmost methylene protons adjacent to the peripheral amines of F-PAMAM dendrimer shifted downfield to 2.97 ppm. Evidently, this was due to an electron-withdrawing effect from the terminal cationic amines which had been fully protonated by APS treatment. The pH values for PAMAM and F-PAMAM dendrimer solutions were found to be 10.1 and 8.5, respectively, again confirming that the terminal primary amines with a pK_a value of 9.2 were indeed neutralized by acidic APS reagent (pH ∼ 4).[40]

To further clarify the consequence of APS treatment on observed cytotoxicity, fresh PAMAM dendrimer was doped with two kinds of acidic ammonium salts lacking any oxidizing capability, namely ammonium sulfate and ammonium chloride for cell viability test. As shown in Figure 2, thus-prepared PAMAM dendrimers bearing protonated terminal amines as well had certain toxicity toward C6 cells; and also, as expected, the dendrimer solution was incapable of emitting detectable fluorescence. Apparently, APS-promoted oxidation not only induced the nonclassical photoluminescence but also played a key role in decreasing the cytotoxicity of F-PAMAM dendrimer. The mechanism for this observed detoxification effect of oxidized PAMAM dendrimer toward C6 cells remains unclear. However, some researchers have suggested that APS treatment might slightly degrade peripheral amines via the Cope elimination reaction and, thus, diminish the surface charge density and cytotoxicity.[41] Mechanistic studies regarding this unusual issue are currently underway.

The in vitro cytotoxicity of F-PAMAM and AS-ODN complexes was also examined using MTT assay. Three different AS-ODN sequences (p75, NGF1, and NGF2) for knocking down the expression of either p75 neurotrophin receptor or nerve growth factor were complexed with PAMAM dendrimers, at various N/P ratios of 10, 15, 20, and 40. Figure 4 shows the

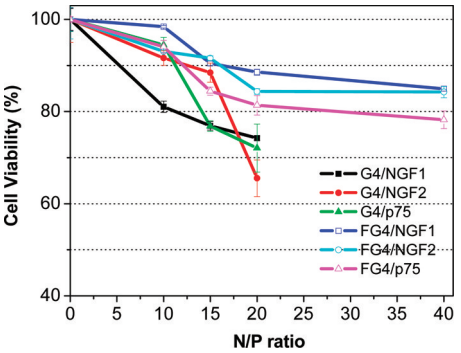

Figure 4. In vitro cytoxocity analyses for the complexes of G4 PAMAM dendrimers and p75, NGF1, and NGF2 AS-ODNs at various N/P ratios. Pristine dendrimer (G4) and NGF1 (■), NGF2 (●), p75 (▲); fluorescent dendrimer (FG4) and NGF1 (□), NGF2 (○), p75 (Δ). The C6 cells were transfected with these complexes for 12 h, and the results are expressed as percentage of cell viability relative to untreated rat C6 glioma cells. Data are the mean ± standard deviation of four experiments, each conducted in triplicate.

viability for C6 cells transfected with these polyplexes for 12 h. More than 80% of cells were viable at the whole range of N/P ratios, for the complexes between F-PAMAM dendrimer and p75, NGF1, and NGF2. However, the N/P ratio for PAMAM/AS-ODN complexes must be carefully manipulated due to the intrinsic high toxicity of NH_2-terminated dendrimer toward C6 cells. Less than 80% of cells survived in the presence of such complexes, at a maximum N/P of 20. This result indicated that the F-PAMAM dendrimer and its AS-ODN complexes had lower toxicity for C6 cell lines. The F-PAMAM dendrimer was, thus, a superior carrier for delivering nucleic acids toward cell lines that were highly sensitive to NH_2-containing polymer vectors. Most importantly, the cytotoxicity of PAMAM-NH_2 dendrimer could be substantially reduced by simply doping with APS reagent, rather than using complicated chemical modification procedures.

Cellular Uptake of F-PAMAM Dendrimer and AS-ODN Complexes. To visualize the cellular uptake of dendrimer−oligonucleotide conjugates, it is necessary to attach a fluorescent label onto either nucleic acids or the dendritic scaffold. In the current study, the intrinsic fluorescence of F-PAMAM and AS-ODN complexes allowed us to omit this routine labeling and to evaluate directly the uptake process via fluorescence techniques. The fluorescent microscopic images shown in Figure 5a,b revealed that the F-PAMAM/p75 complexes could be successfully taken up by C6 cells transfected for 12 h. Although intensity and sharpness of these fluorescent cells were incomparable with conventional

dx.doi.org/10.1021/bm201196p | Biomacromolecules 2011, 12, 4283−4290

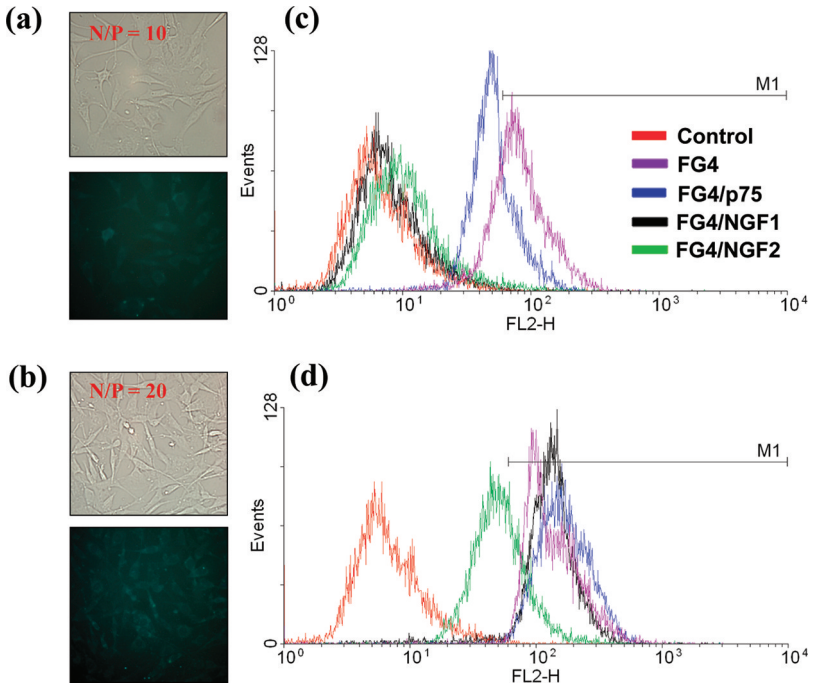

Figure 5. Optical and fluorescence microscopic images of C6 cells transfected with the complexes of fluorescent G4 PAMAM dendrimer (FG4) and p75 AS-ODN at an N/P ratio of 10 (a) and 20 (b). The flow cytometry histograms for counting 1×10^4 cells transfected with p75, NGF1, and NGF2 AS-ODNs delivered by FG4 at an N/P ratio of 20 (c) and 40 (d). The scale bar M1 was established by visual inspection of the histogram of 99% of cells transfected solely with FG4 vector under the concentration of 1.6 μM.

dye-labeled systems, slight intensification of the fluorescent images indicated that the uptake efficiency increased as the N/P ratio increased from 10 to 20. This finding supported the hypothesis that more positive charges for complexes with higher N/P ratios might facilitate the cellular uptake.[42] For delivering AS-ODN, a higher N/P ratio was sometimes necessary to achieve better complexation and cellular uptake; AS-ODN with relatively short sequences and unstable structure usually required more cationic dendrimer carrier than did plasmid DNA. However, the maximum N/P value for pristine PAMAM dendrimer as a safe vector toward C6 cells was found to be 20. Alternatively, F-PAMAM dendrimer may be a superior carrier for shuttling AS-ODN into C6 cells due to its atoxic character at higher N/P ratios.

Flow cytometry with laser irradiation was performed to precisely quantify the cellular uptake efficiency of F-PAMAM/AS-ODN (p75, NGF1, and NGF2) complexes at various N/P ratios for C6 cells.[43] These experiments allowed us to determine the number of cells positive to the fluorescent complexes and the average fluorescence intensity per cell. The flow histograms shown in Figure 5c,d indicated that F-PAMAM dendrimer (alone) and F-PAMAM/p75 complex could be taken up by C6 cells, whereas efficient uptake for F-PAMAM/NGF1 and NGF2 complexes was only observed at an N/P = 40. Figure 6 displays the quantified data in terms of positive cells and mean fluorescence intensity for F-PAMAM dendrimer and its AS-ODN complexes. At N/P = 20, with a dendrimer concentration of 0.8 μM, C6 cells were found to be partially positive (ca. 28%) to F-PAMAM carrying p75 antisense but were hardly stained by F-PAMAM carrying NGF series. When incubated with the vector solely at this concentration, however, more than 80% of cells were positive to the dendrimer. The lower uptake efficiency for the dendrimer associated with AS-ODN is mainly attributed to the formation of larger polyplexes with fewer positive surface charges toward C6 cells. As the N/P ratio further increased to 40, the cells were all positive to the F-PAMAM dendrimer in the presence of p75 and NGF1, but revealed moderate uptake efficiency (ca. 35%) for the complex with NGF2. Moreover, the mean fluorescence intensity of each complex at various N/P ratios (Figure 6b) confirmed the relatively lower uptake efficiency of NGF2 antisense even when the N/P ratio was 40. These results not only suggested that higher N/P values are necessary for delivering short AS-ODN into target cells, but also implied that uptake efficiency strongly depends on the type of oligonucleotides shuttled by the F-PAMAM dendrimer. To our knowledge, this is the first quantified data to evaluate AS-ODN delivery behavior, using an intrinsically fluorescent dendrimer to perform the dual functions of gene carrier and fluorescence probe.

Because p75, NGF1, and NGF2 antisenses have the same number of base pairs and quite similar molecular weights, the distinct uptake behavior of these complexes is attributed to the sequence of the nucleotide residues. These sequences may cause different association patterns between the dendrimer and the oligonucleotides at defined N/P ratios. We used AFM analysis to further examine the morphology of these complexes composed of F-PAMAM dendrimer and AS-ODN. As shown in Figure 7, the electrostatic complexes of dendrimer and p75, which show relatively higher uptake efficiency for C6 cells, revealed well-condensed spherical particles between 160 and 190 nm at N/P of 20. In contrast, NGF2 and F-PAMAM dendrimer only formed amorphous large aggregates at the same N/P ratio. This result was consistent with the quantified data obtained from flow cytometry. These findings suggest that a tailor-made size and shape of the complex at an optimized N/P ratio could facilitate the cellular uptake.[6,44] The use of the intrinsic fluorescent property of PAMAM dendrimers and bioimaging techniques allow for the detection of dissimilar uptake behavior of these complexes, consequently determining an optimized N/P ratio for delivering different oligonucleotides toward target cells.

dx.doi.org/10.1021/bm201196p | *Biomacromolecules* 2011, 12, 4283–4290

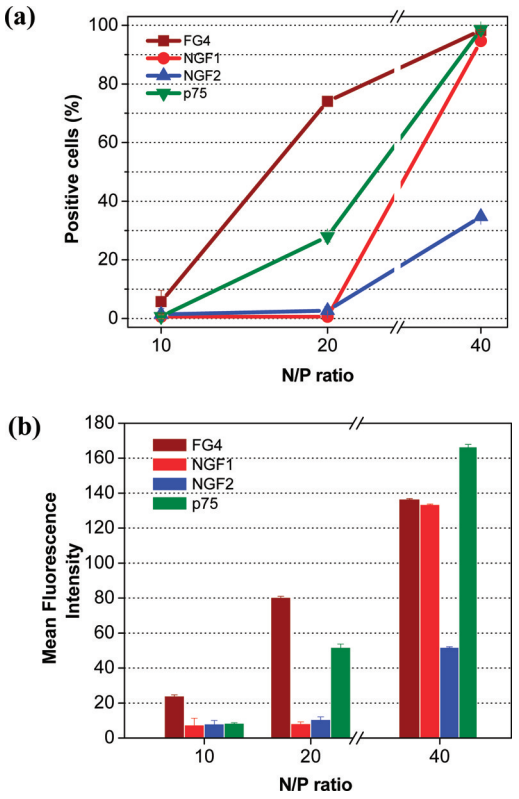

Figure 6. (a) Percentage of positive cells and (b) the mean fluorescence intensity of cells for the fluorescent complexes of fluorescent G4 PAMAM dendrimer (FG4; ■) and NGF1 (●), NGF2 (▲), p75 (▼) AS-ODNs at N/P ratios of 10, 20, and 40, where the dendrimer concentrations equal 0.4, 0.8, and 1.6 μM, respectively. The positive fluorescence level was based on the scale bar M1 established by visual inspection of the flow cytometry histogram of 99% of cells transfected solely with FG4 vector under the concentration of 1.6 μM.

In Vitro Transfection and p75NTR/NGF Protein Knockdown by F-PAMAM/AS-ODN Complexes. According to the "proton sponge" hypothesis, the buffering capacity presented by PAMAM dendrimers with internal tertiary amines leads to osmotic swelling and rupture of endosomes. This process results in the release of the AS-ODN into cytoplasm for gene transfection. To examine F-PAMAM/AS-ODN complexes that had been internalized into C6 cells, we used Western blotting method to analyze gene transfection of p75 and NGF antisenses, in terms of their protein knock-down capability. As shown in Figure 8, compared with a control group (i.e., AS-ODN without vector), the dendrimers carrying different antisenses toward the inhibition of specific protein expression exhibited charge-ratio-dependent knockdown efficiency. This finding suggests that a higher N/P ratio facilitated the in vitro transfection. We also noted that p75 and NGF1 had higher

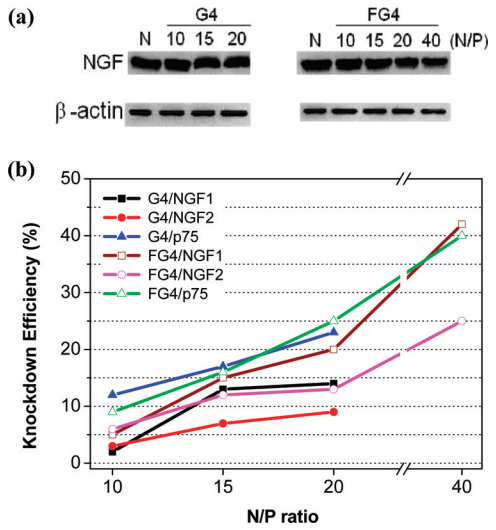

Figure 8. (a) Western blot analysis of NGF and β-actin (internal control) protein expression after C6 cell transfection with the complexes of G4 PAMAM dendrimer and NGF1 AS-ODN at various N/P ratios. (b) Summarized data for NGF and p75NTR protein knock-down efficiency after C6 cell transfection with NGF1, NGF2, and p75 AS-ODNs delivered by G4 PAMAM dendrimer. Pristine dendrimer (G4) and NGF1 (■), NGF2 (●), p75 (▲); fluorescent dendrimer (FG4) and NGF1 (□), NGF2 (○), p75 (Δ).

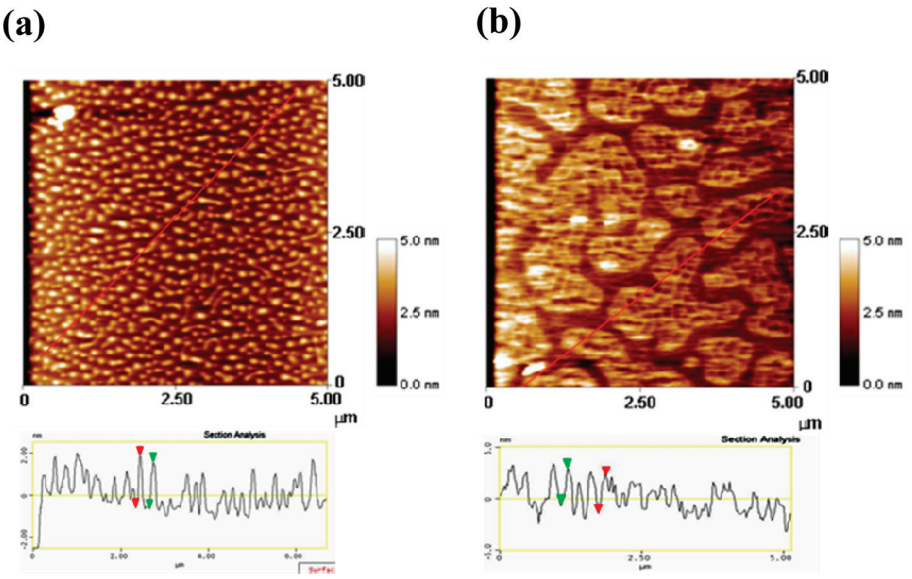

Figure 7. Atomic force microscopic (AFM) images and their corresponding surface profiles for the complexes of fluorescent G4 PAMAM dendrimer with (a) p75 and (b) NGF2 AS-ODNs at N/P = 20.

dx.doi.org/10.1021/bm201196p | *Biomacromolecules* 2011, 12, 4283–4290

efficiency than NGF2 to knock down the corresponding p75NTR and NGF protein expression. This result was consistent with the cellular uptake profile of different F-PAMAM/AS-ODN complexes quantified by flow cytometry; that is, higher uptake level accounts for better gene transfer activity. Moreover, among three antisenses delivered by either pristine PAMAM or F-PAMAM dendrimer, the inhibition of p75NTR protein expression had optimized knockdown efficiency (ca. 23−25%) at an N/P = 20. However, due to its less toxic character, F-PAMAM dendrimer is capable of delivering both p75 and NGF1 antisenses into C6 cells with even higher transfection efficiency (ca. 40−42%) at an N/P ratio of 40, with more than 80% of cells still being viable. Although the optimized p75 transfection mediated by F-PAMAM dendrimer and hyperbranched PEI had comparable efficiency (Figure S2), the former is definitely a secure vector for C6 glioma cells.

CONCLUSIONS

In summary, the delivery of three AS-ODNs, namely, p75, NGF1, and NGF2, into rat C6 glioma cell lines was successfully carried out using intrinsic fluorescent PAMAM dendrimer as a nonviral gene carrier. The NH_2-terminated G4 PAMAM dendrimer was readily treated with an oxidizing reagent to yield blue fluorescence with moderate quantum yield. This allowed us to straight evaluate the dendrimer-mediated delivery and cellular uptake by fluorescence microscopy and flow cytometry, without using fluorescent labeling. The quantitative results clearly suggested dissimilar uptake efficiency as a sequence of p75 > NGF antisense shuttled by the fluorescent dendrimer at the same N/P value. AFM analysis confirmed that this distinct uptake behavior is mainly due to the association patterns between dendrimer and the oligonucleotide sequences of different nucleotide residues. Our findings suggest that the tailor-made size and shape of the complex at an optimized N/P ratio facilitate the cellular uptake. Furthermore, compared with the highly cytotoxic polyamine vectors for C6 cells, the oxidative PAMAM dendrimer (bearing unexpected lower cytotoxicity) could afford more efficient in vitro transfection at a higher dendrimer-to-AS-ODN (N/P) feeding ratio, thus facilitating the down-regulation of specific protein expression to a level comparable to hyperbranched PEI-meditated delivery and transfection. Taking all of our findings into account, we expected that intrinsically fluorescent PAMAM dendrimers may combine the multiple functions of delivery, imaging, and transfection into a single gene vehicle, which has considerable potential for antisense technology. Although much can be done in the future to further improve the fluorescence properties toward in vitro and in vivo imaging, we also anticipate this less toxic material combined targeting peptides ligation can serve as a novel nanoplatform for cancer imaging and therapy.

ASSOCIATED CONTENT

Supporting Information

Experimental conditions of PEI-mediated delivery and the data for in vitro cytotoxicity and gene transfection. This material is available free of charge via the Internet at http://pubs.acs.org.

AUTHOR INFORMATION

Corresponding Author

*Tel./Fax: +886-4-2324-8189. E-mail: jrchu@csmu.edu.tw.

ACKNOWLEDGMENTS

C.-C.C. would like to thank Chung Shan Medical University and the National Science Council of Taiwan, Republic of China, for financially supporting this research (NSC98-2113-M-040-003-MY2). Flow cytometry was performed in the Instrument Center of Chung Shan Medical University, which is supported by the National Science Council, Ministry of Education, and Chung Shan Medical University.

REFERENCES

(1) Takahashi, Y.; Nishikawa, M.; Takakura, Y. *Adv. Drug Delivery Rev.* **2009**, *61*, 760−766.
(2) Gao, K.; Huang, L. *Mol. Pharmacol.* **2009**, *6*, 651−658.
(3) Shery, K.; Suchit, A.; Nishant, M.; Vibha, R. *Biochem. Biophys. Res. Commun.* **2009**, *386*, 273−277.
(4) Fattal, E.; Barratt, G. *Br. J. Pharmacol.* **2009**, *157*, 179−194.
(5) Gary, D. J.; Puri, N.; Won, Y. Y. *J. Controlled Release* **2007**, *121*, 64−73.
(6) Froehlich, E.; Mandeville, J. S.; Weinert, C. M.; Kreplak, L.; Tajmir-Riahi, H. A. *Biomacromolecules* **2011**, *12*, 511−517.
(7) Fant, K.; Esbjörner, E. K.; Jenkins, A.; Grossel, M. C.; Lincoln, P.; Nordén, B. *Mol. Pharm.* **2010**, *7*, 1734−1746.
(8) Yuan, Q.; Yeudall, A.; Yang, H. *Biomacromolecules* **2010**, *11*, 1940−1947.
(9) Mintzer, M. A.; Simanek, E. E. *Chem. Rev.* **2009**, *109*, 259−302.
(10) Arima, H.; Motoyama, K. *Sensors* **2009**, *9*, 6346−6361.
(11) Ravina, M.; Paolicelli, P.; Seijo, B.; Sanchez, A. *Mini-Rev. Med. Chem.* **2010**, *10*, 73−86.
(12) Patil, M. L.; Zhang, M.; Betigeri, S.; Taratula, O.; He, H.; Minko, T. *Bioconjugate Chem.* **2008**, *19*, 1396−1403.
(13) Tsutsumi, T.; Hirayama, F.; Uekama, K.; Arima, H. *J. Controlled Release* **2007**, *119*, 349−359.
(14) Zhou, J.; Wu, J.; Hafdi, N.; Behr, J.-P.; Erbacher, P.; Peng, L. *Chem. Commun.* **2006**, 2362−2364.
(15) Bielinska, A.; Kukowska-Latallo, J. F.; Johnson, J.; Tomalia, D. A.; Baker, J. R. Jr. *Nucleic Acids Res.* **1996**, *24*, 2176−2182.
(16) Sonawane, N. D.; Szoka, F. C. Jr.; Verkman, A. S. *J. Biol. Chem.* **2003**, *278*, 44826−44831.
(17) Wang, W.; Xiong, W.; Wan, J.; Sun, X.; Xu, H.; Yang, X. *Nanotechnology* **2009**, *20*, 105103−105109.
(18) Kim, Y.; Klutz, A. M.; Jacobson, K. A. *Bioconjugate Chem.* **2008**, *19*, 1660−1672.
(19) Kolhatkar, R. B.; Kitchens, K. M.; Swaan, P. W.; Ghandehari, H. *Bioconjugate Chem.* **2007**, *18*, 2054−2060.
(20) Majoros, I. J.; Myc, A.; Thomas, T.; Mehta, C. B.; Baker, J. R. Jr. *Biomacromolecules* **2006**, *7*, 572−579.
(21) Patri, A. K.; Myc, A.; Beals, J.; Thomas, T. P.; Bander, N. H.; Baker, J. R. Jr. *Bioconjugate Chem.* **2004**, *15*, 1174−1181.
(22) Yoo, H.; Juliano, R. L. *Nucleic Acids Res.* **2000**, *28*, 4225−4231.
(23) Barret, T.; Ravizzini, G.; Choyke, P. L.; Kobayashi, H. *IEEE Eng. Med. Biol. Mag.* **2009**, *28*, 12−22.
(24) Lee, W. I.; Bae, Y.; Bard, A. J. *J. Am. Chem. Soc.* **2004**, *126*, 8358−8359.
(25) Wang, D.; Imae, T. *J. Am. Chem. Soc.* **2004**, *126*, 13204−13205.
(26) Jasmine, M. J.; Prasad, E. *J. Phys. Chem. B* **2010**, *114*, 7735−7742.
(27) Jasmine, M. J.; Kavitha, M.; Prasad, E. *J. Lumin.* **2009**, *129*, 506−513.
(28) Chen, Y.; Zhou, L.; Pang, Y.; Huang, W.; Qiu, F.; Jiang, X.; Zhu, X.; Yan, D.; Chen, Q. *Bioconjugate Chem.* **2011**, *22*, 1162−1170.
(29) Yang, W.; Pan, C. Y.; Liu, X. Q.; Wang, J. *Biomacromolecules* **2011**, *12*, 1523−1531.
(30) Biswal, B. K.; Kavitha, M.; Verma, R. S.; Prasad, E. *Cytotechnology* **2009**, *61*, 17−24.
(31) Al-Jamal, K. T.; Ruenraroengsak, P.; Hartell, N.; Florence, A. T. *J. Drug Targeting* **2006**, *14*, 405−412.
(32) Weis, C.; Wiesenhofer, B.; Humpel, C. *J. Neuro-Oncol.* **2002**, *56*, 59−67.

(33) Qaiser, A. A.; Hyland, M. M.; Patterson, D. A. *J. Phys. Chem. B* **2009**, *113*, 14986−14993.
(34) Mazur, M. *J. Phys. Chem. C* **2008**, *112*, 13528−13534.
(35) Gall, J. F.; Church, G. L.; Brown, R. L. *J. Phys. Chem.* **1943**, *47*, 645−649.
(36) Saravanan, G.; Imae, T. *J. Nanosci. Nanotechnol.* **2011**, *11*, 4838−4845.
(37) Chu, C. C.; Imae, T. *Macromol. Rapid Commun.* **2009**, *30*, 89−93.
(38) Mosmann, T. *J. Immunol. Methods* **1983**, *65*, 55−63.
(39) Hong, S.; Rattan, R.; Majoros, I. J.; Mullen, D. G.; Peters, J. F.; Shi, X.; Bielinska, A. U.; Blanco, L.; Orr, B. G.; Baker, J. R. Jr.; Holl, M. M. B. *Bioconjugate Chem.* **2009**, *20*, 1503−1513.
(40) Leisner, D.; Imae, T. *J. Phys. Chem. B* **2003**, *107*, 13158−13167.
(41) Lin, S. Y.; Wu, T. H.; Jao, Y. C.; Liu, C. P.; Lin, H. Y.; Lo, L. W.; Yang, C. S. *Chem.—Eur. J.* **2011**, *17*, 7158−7161.
(42) Nomani, A.; Haririan, I.; Rahimnia, R.; Fouladdel, S.; Gazori, T.; Dinarvand, R.; Omidi, Y.; Azizi, E. *Int. J. Nanomed.* **2010**, *5*, 359−369.
(43) Kang, C.; Yuan, X.; Li, F.; Pu, P.; Yu, S.; Shen, C.; Zhag, Z.; Zhang, Y. *J. Biomed. Mater. Res., Part A* **2010**, *93A*, 585−594.
(44) Mitra, A.; Imae, T. *Biomacromolecules* **2004**, *5*, 69−73.